



HAL
open science

Multiplexed Biosensing and Bioimaging Using Lanthanide-Based Time-Gated Förster Resonance Energy Transfer

Xue Qiu, Jingyue Xu, Marcelina Cardoso dos Santos, Niko Hildebrandt

► **To cite this version:**

Xue Qiu, Jingyue Xu, Marcelina Cardoso dos Santos, Niko Hildebrandt. Multiplexed Biosensing and Bioimaging Using Lanthanide-Based Time-Gated Förster Resonance Energy Transfer. *Accounts of Chemical Research*, 2022, 55 (4), pp.551-564. 10.1021/acs.accounts.1c00691 . hal-03594915

HAL Id: hal-03594915

<https://normandie-univ.hal.science/hal-03594915>

Submitted on 26 Jan 2023

HAL is a multi-disciplinary open access archive for the deposit and dissemination of scientific research documents, whether they are published or not. The documents may come from teaching and research institutions in France or abroad, or from public or private research centers.

L'archive ouverte pluridisciplinaire **HAL**, est destinée au dépôt et à la diffusion de documents scientifiques de niveau recherche, publiés ou non, émanant des établissements d'enseignement et de recherche français ou étrangers, des laboratoires publics ou privés.

Multiplexed biosensing and bioimaging using lanthanide-based time-gated FRET

Xue Qiu,^{1,2*} Jingyue Xu,³ Marcelina Cardoso Dos Santos,⁴ and Niko Hildebrandt^{3,5,6*}

¹ School of Medicine and Pharmacy, Ocean University of China, 266003 Qingdao, China.

² Laboratory for Marine Drugs and Bioproducts of Qingdao National Laboratory for Marine Science and Technology, 266237 Qingdao, China.

³ nanofret.com, Laboratoire COBRA, Université de Rouen Normandie, Normandie Université, CNRS, INSA Rouen, 76000 Rouen, France.

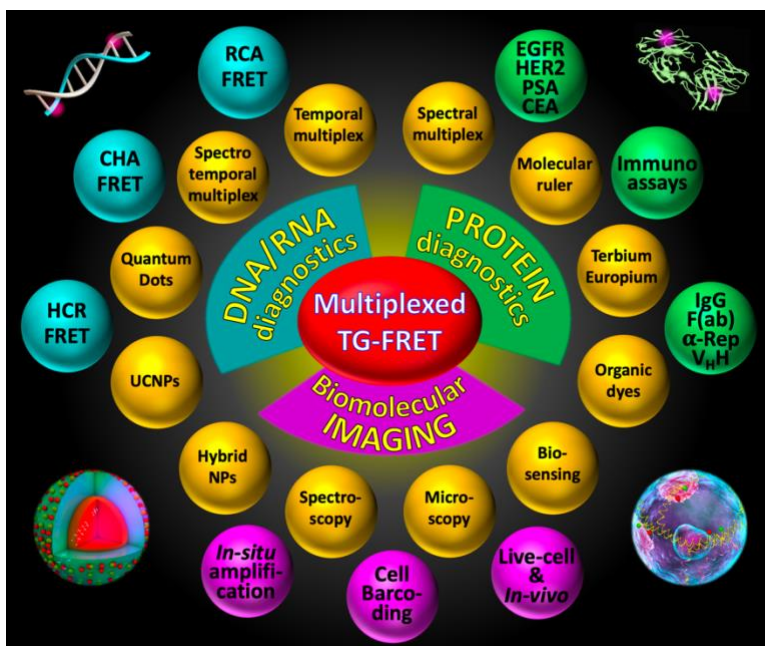
⁴ Institute for Integrative Biology of the Cell (I2BC), Université Paris-Saclay, CEA, CNRS, 91198 Gif-sur-Yvette, France

⁵ Department of Chemistry, Seoul National University, Seoul 08826, South Korea.

⁶ Université Paris-Saclay, 91405 Orsay Cedex, France.

*e-mail: giuxue@ouc.edu.cn; niko.hildebrandt@univ-rouen.fr

CONSPECTUS: The necessity to scrutinize more and more biological molecules and interactions both in solution and on the cellular level has led to an increasing demand for sensitive and specific multiplexed diagnostic analysis. Photoluminescence (PL) detection is ideally suited for multiplexed biosensing and bioimaging because it is rapid and sensitive and there is an almost unlimited choice of fluorophores that provide a large versatility of photophysical properties, including PL intensities, spectra, and lifetimes.



The most frequently used technique to detect multiple parameters from a single sample is spectral (or color) multiplexing with different fluorophores, such as organic dyes, fluorescent proteins (FPs), quantum dots (QDs), or lanthanide nanoparticles and complexes. In conventional PL biosensing approaches, each fluorophore requires a distinct detection channel and excitation wavelength. This drawback can be overcome by Förster resonance energy transfer (FRET) from lanthanide donors to other fluorophore acceptors. The lanthanides' multiple and spectrally narrow emission bands over a broad spectral range can overlap with several different acceptors at once, thereby allowing FRET from one donor to multiple acceptors. The lanthanides' extremely long PL lifetimes provide two important features. First, time-gated (TG) detection allows for efficient suppression of background fluorescence from the biological environment or directly excited acceptors. Second, temporal multiplexing, for which the PL lifetimes are adjusted by the interaction with the FRET acceptor, can be used to determine specific biomolecules and/or their conformation via distinct PL decays. The high signal-to-background ratios, reproducible and precise ratiometric and homogeneous (washing-free) sensing formats, and higher-order multiplexing capabilities of lanthanide-based TG-FRET have resulted in significant advances in the analysis of biomolecular recognition. Applications range from the fundamental analysis of biomolecular interactions and conformations, over high-throughput and point-of-care *in-vitro* diagnostics and DNA sequencing, to advanced optical encoding, using both liquid and solid samples and *in-situ*, *in-vitro*, and *in-vivo* detection with high sensitivity and selectivity.

In this Account, we discuss recent advances of lanthanide-based TG-FRET for the development and application of advanced immunoassays, nucleic acid sensing, and fluorescence imaging. In addition to the different spectral and temporal multiplexing approaches, we highlight the importance of a careful design and combination of different biological, organic, and inorganic molecules and nanomaterials for an adjustable FRET donor-acceptor distance that determines the ultimate performance of the diagnostic assays and conformational sensors in their physiological environment. We conclude by sharing our vision on how progress in the development of new sensing concepts, material combinations, and instrumentation can further advance TG-FRET multiplexing and accelerate a translation into routine clinical practice and the investigation of challenging biological systems.

KEY REFERENCES:

- Léger, C., Yahia-Ammar, A., Susumu, K., Medintz, I. L., Urvoas, A., Valerio-Lepiniec, M., Minard, P., and Hildebrandt, N. Picomolar Biosensing and Conformational Analysis Using Artificial Bidomain Proteins and Terbium-to-Quantum Dot Förster Resonance Energy Transfer. *ACS Nano* **2020**, *14*(5), 5956–5967.¹ A Tb-QD TG-FRET pair was assembled on an α -Rep bidomain to quantify the conformational change during target binding and the target concentration within one measurement under physiological conditions.
- Qiu, X., Guo, J., Xu, J., and Hildebrandt, N. Three-Dimensional FRET Multiplexing for DNA Quantification with Attomolar Detection Limits. *J. Phys. Chem. Lett.* **2018**, *9*, 4379–4384.² Spectrotemporal multiplexing (PL color and lifetime) for the detection of attomolar DNA concentrations by RCA-TG-FRET with Tb-donor and dye-acceptor DNA probes.
- Chen, C., Corry, B., Huang, L., and Hildebrandt, N. FRET-Modulated Multihybrid Nanoparticles for Brightness-Equalized Single-Wavelength Barcoding. *J. Am. Chem. Soc.* **2019**, *141*(28), 11123–11141.³ Multistep FRET from Tb-to-QD-to-dye, all assembled in one single nanohybrid, for the production of brightness-equalized multiplexed TG-FRET imaging probes with one excitation and one emission wavelength.
- Cardoso Dos Santos, M., Colin, I., Ribeiro Dos Santos, G., Susumu, K., Demarque, M., Medintz, I.L., and Hildebrandt, N. Time-gated FRET nanoprobe for autofluorescence-free long-term in vivo imaging of developing zebrafish. *Adv. Mater.* **2020**, *32* (39), 2003912.⁴ Tb-to-QD TG-FRET nanohybrids for intracellular multiplexing, binding to intracellularly expressed FPs, and long-term background-free imaging in developing zebra fish embryos.

1. INTRODUCTION

Although the origins of delayed luminescence detection and FRET date back over 100 years,^{5,6} the field of FRET biosensing started growing in the 1990s with the development of TG-FRET immunoassays,⁷ commercial lanthanide-based TG-FRET immunoassays,⁸ FRET DNA sequencing,⁹ FRET with FPs,¹⁰ and single-pair FRET,¹¹ to name only a few. Over the last 20 years, new fluorophores, such as QDs or other nanomaterials,^{12,13} had a large influence on the development of advanced FRET sensing concepts, including their combination with lanthanides for TG-FRET.^{12,14,15} The traditional advantages of TG-FRET are high spatial resolution, ratiometric and washing-free sensing formats, and efficient background-suppression.¹⁶⁻¹⁹ These unique features of TG-FRET result in high sensitivity, specificity, and simplicity, all of which are paramount for advanced biosensing and bioimaging. The versatility of combining various optically and biologically active materials and tuning their interaction via size, number, color, conformation, and proximity for the development of new multiplexing concepts, is a remarkable hallmark of TG-FRET, whose recent advances we discuss in this Account.

2. MULTIPLEXED TIME-GATED FRET

Lanthanide (*e.g.*, Tb or Eu) complexes are interesting FRET donors because they possess relatively large PL quantum yields, extremely long PL lifetimes, and multiple narrow emission bands over a broad spectral range.^{19,20} Using FRET acceptors with specific fluorescence colors and placing them at controlled distances to the lanthanide FRET donor, gives access to both spectral (color) and temporal (lifetime) PL multiplexing, which can be combined into higher-order multiplexed and quantitative biosensing and bioimaging.

2.1. *FRET distance control*

Donor-acceptor distance is one of the most important parameters in FRET and a well-controlled distance is a prerequisite for efficient FRET.²¹ The well-defined structures of biomolecules are natural resources for a specific donor-acceptor separation via controlled bioconjugation.²² Moreover, they can also be used for the specific recognition of many biological and chemical targets and analytes. Modification of nucleic acids with fluorophores or functional bioconjugation groups at distinct positions is commercially available at many vendors. Proteins engineered with unnatural amino acids,²³ amino acid sequence recognized by enzymes,²⁴ or single cysteines²⁵ can also be site-specifically labeled with fluorophores. The much simpler structure of nucleic acids

makes distance control significantly more straightforward compared to proteins. The same holds true for small fluorophores (*e.g.*, dyes and lanthanide complexes) compared to relatively large nanoparticles (*e.g.*, QDs). In addition to structure and size, shape and orientation of biomolecules and fluorophores must be considered for controlling FRET.

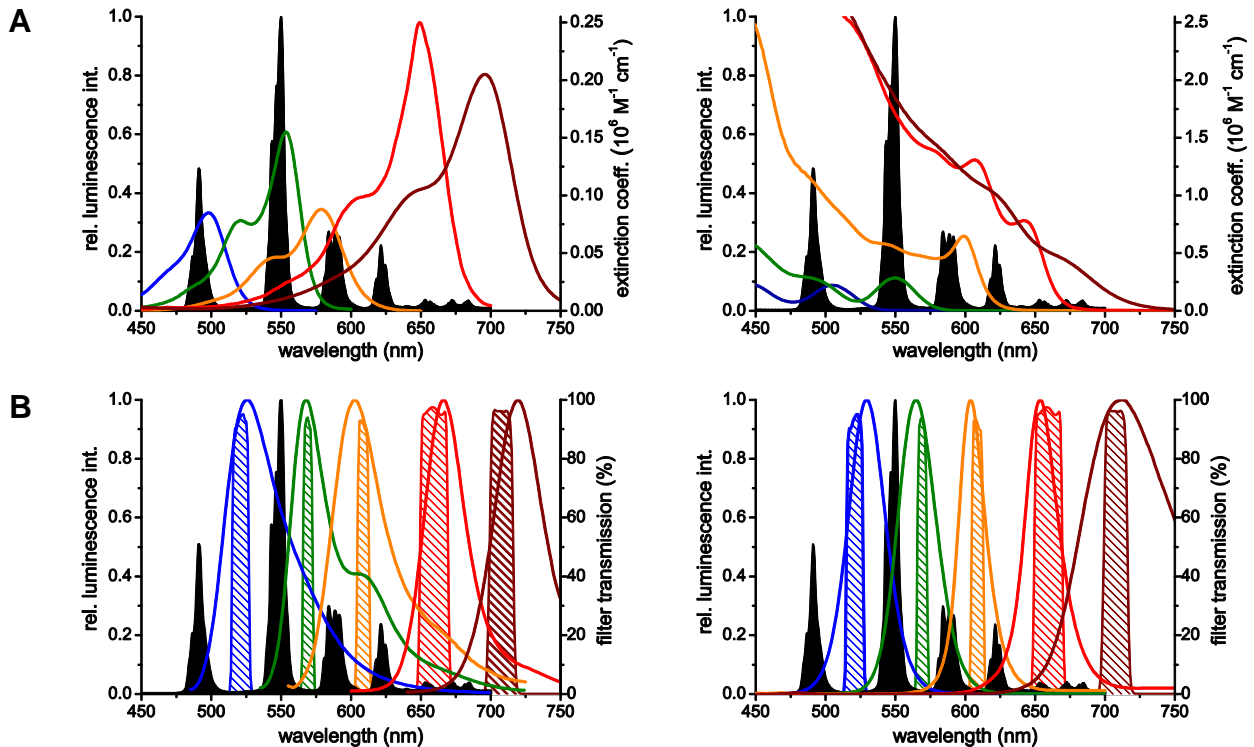
2.2. Spectral (PL color) multiplexing

The distinct PL spectra of different lanthanide complexes can be efficiently used for color multiplexing.²⁶ For FRET multiplexing, Tb has the advantage of better-separated emission bands (compared to Eu), which are particularly well suited to be combined with differently colored acceptors, such as dyes or QDs (**Figure 1A**).¹⁴ The spectral range of acceptor fluorescence is mainly limited by the spectral overlap of acceptor absorption and lanthanide donor emission and starts around 500 nm (after the first emission band of Tb - cf. **Figure 1A** and **1B**). In particular, for QDs, orange to red emitting QDs are preferred because of their much broader spectral overlap (**Figure 1A** right). In a typical spectrally multiplexed TG-FRET measurement, TG PL intensities are collected in different donor and acceptor emission channels (**Figure 1B**). Spectral separation distinguishes the different FRET-sensitized acceptors and the FRET-quenched Tb donor. TG detection suppresses short-lived PL from sample autofluorescence or from acceptors that were directly excited by the excitation pulse. When the different acceptor PL spectra overlap within the distinct detection channels (*e.g.*, due to the relatively broad PL spectra of dyes), so-called spectral crosstalk correction can be used to improve multiplexing specificity.²⁷ In multiplexed biosensing, each color detection channel is used for one specific target (analyte), which requires sequential measurements or multiple detectors.

2.3. Temporal (PL lifetime) multiplexing

The very long PL lifetimes of lanthanides are an excellent basis for FRET distance control. Double-stranded (ds)DNA is quite rigid and Tb-to-dye or Tb-to-QD distances can be adjusted with a resolution of *circa* 0.31 nm to 0.34 nm per base pair.^{28,29} Single-stranded (ss)DNA is less rigid and, depending on the environmental conditions, a denser conformation can be found, *e.g.*, with ~0.15 nm per base when Tb is attached via ssDNA on QD surfaces.²⁹ Despite their more complex structures, proteins can also be used to adjust Tb-to-QD donor acceptor distances.¹ QD surface coatings with defined thicknesses are another possibility to tune the distance between lanthanides and QDs.^{3,30} The shorter/longer the distance, the shorter/longer the PL lifetime of both the FRET-quenched lanthanide donor and the FRET-sensitized dye or QD acceptor (**Figure 1C**). A

temporally multiplexed biosensor must be designed, such that each target corresponds to a specific donor-acceptor distance and thus, a specific PL decay curve with a specific PL lifetime. In a typical measurement (**Figure 1D**), PL intensities of the FRET-sensitized acceptor are collected in multiple TG detection windows (*e.g.*, 0.02 to 1.5 ms, 1.5 to 4.0 ms, and 4.0 to 8.0 ms after the excitation pulse) that can all be extracted from a single PL decay curve (one measurement for all TG detection windows). The multiplexed biosensor is calibrated by first quantifying the acceptor PL contributions for each single target within each TG detection window. For multiplexing, the PL contribution of each target within the different TG windows can be deconstructed by a straightforward matrix calculation.²⁸ The temporal widths of the detection windows must be adapted to the PL decay curves and the number of windows should be equal to that of the targets. The method only uses TG PL intensities and does not require PL lifetime analysis. Because the complete PL decay curve is collected within one measurement, temporal multiplexing does not require sequential measurements or multiple detectors. Moreover, only a single FRET pair is required. On the downside, the complete PL intensity is divided into different fractions and there are contributions from multiple PL decay curves in the different TG detection windows. Therefore, biosensing with temporal multiplexing is usually less sensitive than with spectral multiplexing.



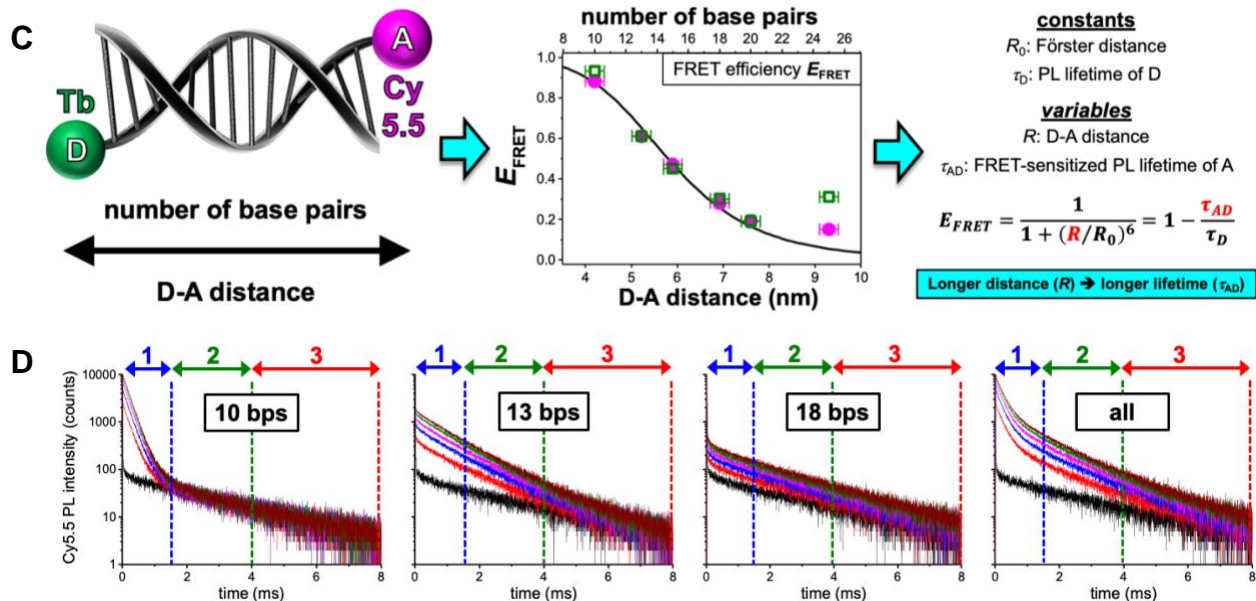


Figure 1. Spectral and temporal FRET multiplexing. (A) Spectral overlap between the emission of one Tb donor (black) and the absorption of five different dye (left) or QD (right) acceptors (colored). (B) The spectral separation of PL from Tb donors (black) and from dye (left) or QD (right) acceptors permits multiplexed PL color detection via different bandpass filters (striped transmission spectra). A and B reproduced with permission from ref. 14. Copyright 2014 Elsevier. (C) Tuning the donor-acceptor (D-A) distance by the number of DNA base pairs (left), results in a D-A distance-dependent FRET efficiency (center) and a concomitant D-A distance-dependent PL lifetime of the FRET donor and acceptor (right). (D) PL decay curves of FRET-sensitized Cy5.5 dyes separated by 10, 13, or 18 base pairs (bps) from the Tb donor. The different TG detection windows (1 - blue; 2 - green; 3 - red) can be simultaneously extracted from each single PL decay curve. Different intensities represent the target concentrations (0 to 3 nM from black to brown). C and D adapted with permission from ref. 28. Copyright 2017 Wiley.

2.4. Spectrotemporal (combined color and lifetime) multiplexing

Spectral and temporal multiplexing can be combined into spectrotemporal multiplexing with different PL colors (several acceptors) and different PL lifetimes (different donor-acceptor distances) (**Figure 2**).² In this so-called higher-order multiplexing, the number of distinguishable targets is the product $a \times b$ when all targets are mixed within a sample or the exponentiation a^b when targets can be spatially separated, with a and b being the number of distinguishable acceptors (color) and PL decay curves (lifetime), respectively. Although theoretically a and b can be very large numbers, the practical limitations of both spectral and temporal multiplexing are also valid for their combination. Considering that efficient TG-FRET multiplexing was experimentally demonstrated with five different QD and dye acceptors and three different PL decay curves,^{27,28,31} spectrotemporal multiplexing with $a = 5$ and $b = 3$ should be practically feasible without significant additional complications when compared to spectral or temporal multiplexing alone. Notably, excitation-wavelength based differentiation of lanthanide complexes should be able to further

extend the spectrotemporal multiplexing capability.^{32,33} Technical implementation of spectrotemporal multiplexing into diagnostic assays should be relatively straightforward, considering that many fluorescence spectrometers and plate readers already provide multiple color channels and TG detection (often referred to as “TR-FRET” or “HTRF” by the different providers).¹⁷

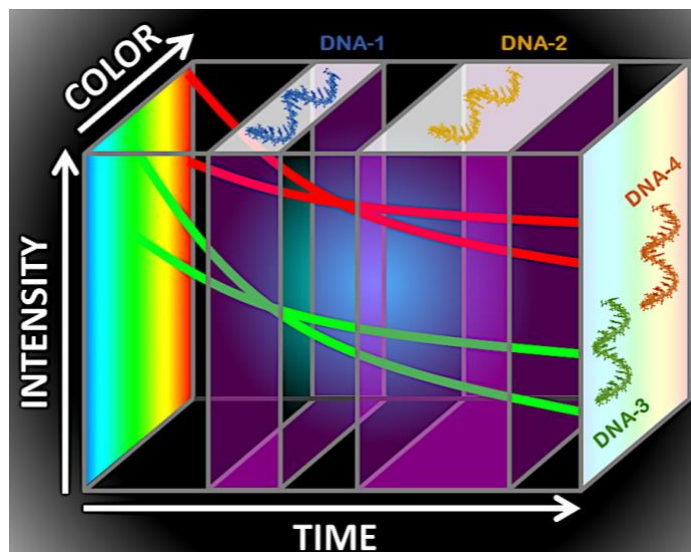


Figure 2. Spectrotemporal FRET multiplexing. Two different PL colors and two different PL decays measured in two temporal detection windows can be combined to quantify the concentrations (via the PL intensity) of four different DNA targets in solution. Reproduced with permission from ref. 2. Copyright 2018 American Chemical Society.

3. TG-FRET IMMUNOASSAYS

TG-FRET immunoassays usually apply two distinct antibodies (one conjugated with a lanthanide-based donor and the other with an appropriate fluorescent acceptor) that separately bind to different epitopes of a target antigen, such that they are in close proximity for FRET. Because TG-FRET-sensitized acceptor PL can only occur upon specific antibody-target-antibody sandwich formation, high signal-to-background ratios can be accomplished without any separation steps. This unique advantage of lanthanide-based TG-FRET has been exploited for many years in highly sensitive and specific assays for *in-vitro* diagnostics, high-throughput drug screening, and the investigation of protein-protein interactions.^{14,16–18}

3.1. Multiplexed detection of tumor markers

The complexity of cancers with various sub-types most often requires the quantification of several tumor markers for specific diagnosis. Multiplexed TG-FRET immunoassay can detect such tumor

marker panels from a single sample. As an example, the distinction between small cell and non-small cell lung carcinoma (SCLC and NSCLC) can be improved by quantifying neuron-specific enolase (NSE), carcinoembryonic antigen (CEA), the cytokeratin-19 fragment Cyfra21-1, squamous cell carcinoma antigen (SCC), and the carbohydrate antigen CA15.3 in human serum.²⁷ Two antibodies against each tumor marker were conjugated with Tb-dye FRET pairs, for which only the dye acceptors were different (**Figure 3A**). Thus, excitation of Tb resulted in FRET to only those dyes contained in antibody-tumor marker-antibody sandwich complexes and their TG PL could be used for specific tumor marker quantification via color multiplexing (**Figure 3B**). For multiplexed quantification from a single sample, each target-specific (color or spectral) detection channel must first be calibrated to obtain signal (e.g., TG acceptor/donor intensity ratio: FRET-ratio) over target concentration curves for each target. These assay calibration curves can then be used to assign the signals from the different detection channels to the different target concentrations.^{2,27,34-40} In addition, the calibration of x channels with y targets can be used to correct for signal and biological crosstalk by multiplying the measured signals by a $x \times y$ correction matrix.^{27,35}

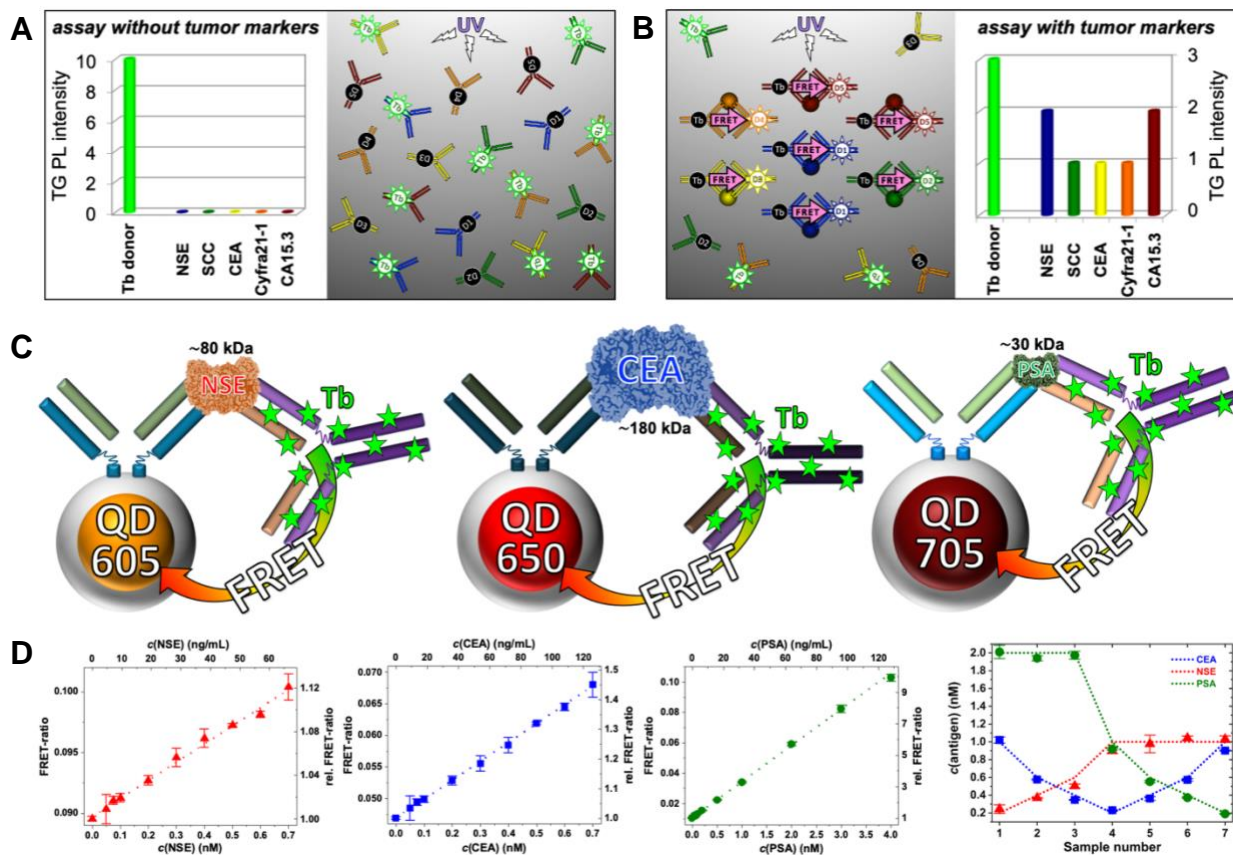


Figure 3. TG-FRET color multiplexing for tumor marker immunoassays. (A) In the absence of tumor markers, Tb excitation results only in Tb PL (no FRET). (B) Formation of specific immunological sandwich complexes results in tumor marker-specific Tb-to-dye TG-FRET. A and B adapted with permission from ref. 27. Copyright 2013 American Chemical Society. (C) Tb-to-QD TG-FRET immunoassays, for which the relatively large sizes of QDs change the acceptor-antibody conjugate. For clarity, only one antibody per QD is shown. Schemes are not to scale. (D) Calibration of the three Tb-QD FRET immunoassays can be used for triplexed tumor marker quantification from a single serum sample. Reproduced with permission from ref. 34. Copyright 2020 The Authors, some rights reserved; exclusive licensee MDPI, Basel, Switzerland. Distributed under a Creative Commons Attribution License 4.0 (CC BY) <https://creativecommons.org/licenses/by/4.0/>.

The same sandwich immunoassay principle can be used with Tb-to-QD FRET and the duplexed quantification of the epidermal growth factor receptors 1 and 2 (EGFR and HER2)⁴¹ or the triplexed detection of CEA, NSE, and prostate specific antigen (PSA).³⁴ Although the strongly reduced spectral crosstalk (**Figure 1B**) is an advantage for color multiplexing, the immunoassay design is more complex because the sizes of QDs are similar to that of the antibodies (**Figure 3C**). Several antibodies can be attached to the surface of one QD, e.g., by covalent binding (with or without crosslinkers) between functional groups on the QD (e.g., maleimides or amines) and the antibody (e.g., free thiols or amino groups) or many other nanobioconjugation strategies.^{34,42–45} Due to a certain variability in the position and flexibility of those functional groups, antibodies can assume different orientations on the QD surface. The donor-acceptor distances are usually larger than with dye-conjugated antibodies and also antigen binding sites may be blocked. As a rule of thumb, we found that complete immunoglobulin G (IgG) antibodies with many Tb donors combined with several smaller antibodies (e.g., reduced F(ab')₂ or Fab') per QD acceptor provided the best sensing performance (**Figure 3D**).⁴²

3.2 Size, orientation, conformation, and proximity for optimizing QD-based immunoassays.

FRET is only functional at donor-acceptor distances (R) below circa 10 nm and the FRET efficiency strongly depends those distances ($\sim R^{-6}$).^{12,16,18} Although Tb-to-QD FRET can extend the FRET distance range and Förster distances (R_0 , for 50% FRET efficiency $R_0 = R$) can range from circa 5 to 11 nm, the sizes of both QDs and antibodies play an important role for TG-FRET assay development. Inorganic QDs are most often in a size range of 4 nm to 12 nm (diameters or ellipsoidal axes) and organic surface coatings can increase their diameters up to 20 nm or more.^{44,46} Antibodies on the QD surface further increase R and thus, smaller alternatives to the relatively large IgGs ($\sim 15 \times 9.5 \times 6 \text{ nm}^3$),⁴¹ such as reduced IgGs (F(ab')₂ or Fab'; $\sim 4 \times 5 \times 8 \text{ nm}^3$ for Fab'),⁴¹ nanobodies (VHH, $\sim 4 \times 2.5 \times 2.5 \text{ nm}^3$),⁴¹ repeat proteins (α Reps; $\sim 5.5 \times 2.5 \times 2.5 \text{ nm}^3$),¹ and albumin-

binding domain-derived affinity proteins (ADAPTs; $1 \times 1.5 \times 2.5 \text{ nm}^3$),⁴⁷ can be attached to the surfaces of QDs (**Figure 4A**).^{1,41,42,47,48} The smaller the antibody, the more of them can be labeled on a QD, thereby providing more biological recognition elements per QD.^{42,44,47,48} Because one QD can be sequentially FRET-sensitized by many lanthanide donors (due to the large difference between lanthanide and QD PL lifetimes), combination with large antibodies (*e.g.*, IgG) labeled with many lanthanide donors can result in Tb-to-QD TG-FRET immunocomplexes with over 200 Tb donors per QD acceptor and a concomitant improvement of the assay performance.⁴² FRET donor-acceptor distance is another important parameter that depends on both the sizes and orientations of the QD-antibody conjugates. For example, conjugation of antibodies via their endogenous disulfide groups on the ZnS shells of compact QDs can result in antigen-binding sites very close to the QD surface and improved TG-FRET immunoassay performance (**Figure 4B**). Many parameters, including size, orientation, labeling ratio, environment, binding affinities, brightness, stability *etc.*, need to be considered and optimized for Tb-to-QD TG-FRET immunoassay development, some of which are summarized in **Supporting Table S1**.

One can also use the target binding-dependent conformational change of a single protein bidomain for biosensing. When α Rep-bidomains are conjugated with a Tb donor on one terminus and attached to a QD acceptor on the other terminus, target binding-induced conformational changes in the α Rep-bidomain result in Tb-QD distance and concomitant FRET efficiency alterations (**Figure 4C**).¹ These conformational changes can be analyzed with sub-nanometer resolution via PL lifetimes (**Figure 4D**) and targets can be quantified at picomolar concentrations via TG-FRET ratios (**Figure 4E**), both using a single measurement at low concentrations in solution and under physiological conditions.

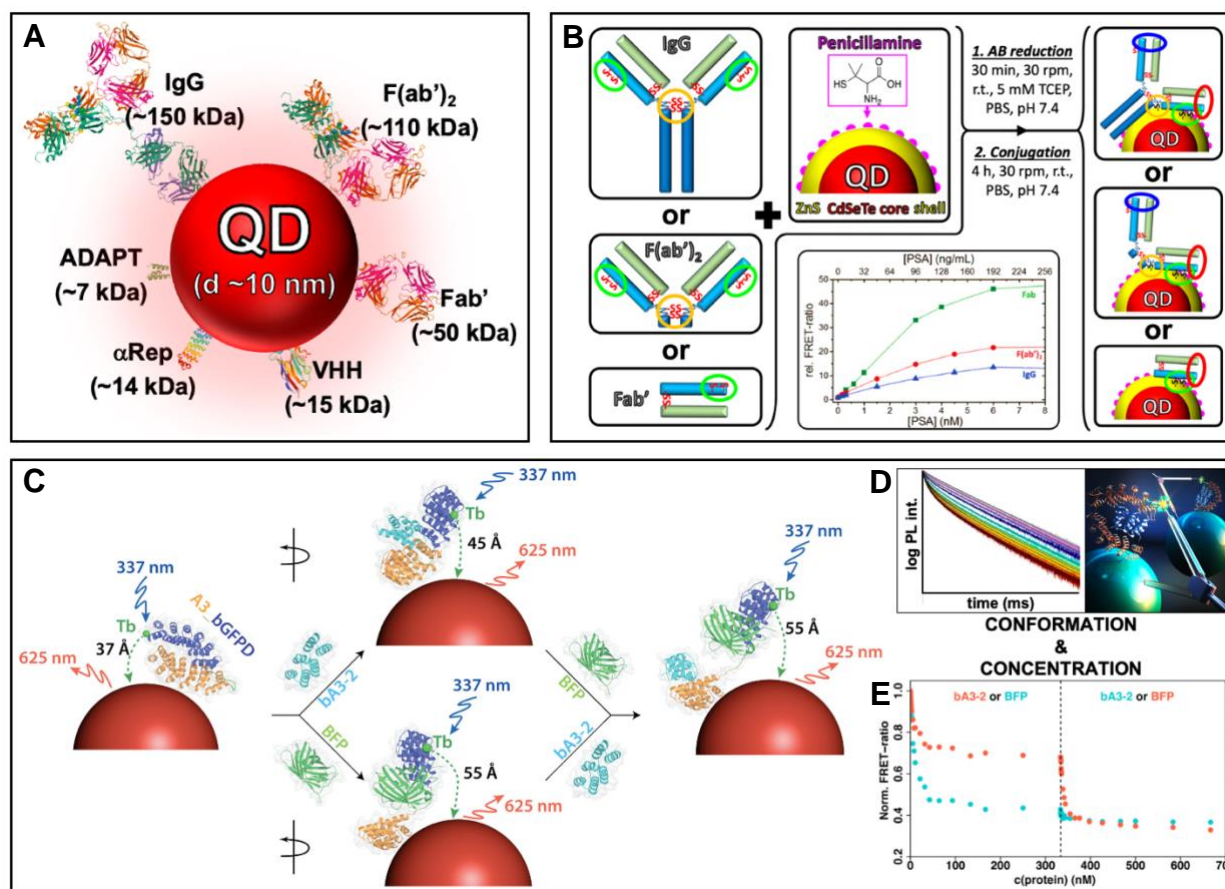


Figure 4. Size and orientation of QD-antibody conjugates. (A) Schematic presentation of biological recognition proteins with various sizes attached to QD surfaces. Protein structures adapted from the RCSB Protein Data Bank (rcsb.org) PDB IDs “1TGT” (for IgG, F(ab)₂, and Fab’), “5IVO” (for VHH), “3LTJ” (αRep), and “1GJT” (ADAPT). (B) Mild reduction of antibody disulfides (green and orange circles) for direct conjugation to QDs. The different orientations result in surface-near and surface-far antigen binding sites (red and blue circles). The smaller the antibody, the better the immunoassay detection performance (assay calibration curve in the center). Adapted with permission from ref. 49. Copyright 2016 The Royal Society of Chemistry. (C) An αRep bidomain (A3_gGFPD) with a Tb donor and QD acceptor leads to Tb-to-QD FRET upon Tb excitation. Depending on target binding of bA3-2 (top), BFP (bottom), or both (right), the bidomain conformation changes. (D) PL decay time analysis can quantify the conformational changes shown in C. (E) TG-FRET ratios of QD and Tb PL can quantify the target concentrations during sequential target-bidomain binding. C to E reproduced with permission from ref. 1. Copyright 2020 American Chemical Society.

4. TG-FRET DNA/RNA HYBRIDIZATION ASSAYS

The structural simplicity of nucleic acids is ideal for designing FRET assays with specific donor-acceptor distances. Therefore, spectral, temporal, and spectrotemporal TG-FRET multiplexing becomes significantly easier compared to protein-based systems. Base-by-base distance adjustment provides sub-nanometer spatial resolution to fine-tune PL lifetimes for TG-FRET temporal

multiplexing or for conformational analysis.^{28,29} Moreover, DNA can be amplified, which gives access to the quantification of extremely low concentrations of DNA or RNA targets even from clinical samples.^{2,36}

4.1 Spectrally multiplexed DNA/RNA hybridization assays

Similar to color multiplexing in sandwich immunoassays, different nucleic acid targets can be quantified by different Tb-dye or Tb-QD FRET pairs. Instead of fluorescent antibody conjugates, fluorescent DNA probes, which get into close proximity upon target hybridization, are used. One example is the multiplexed quantification of micro-RNAs (miRNAs or miRs). Very high target specificity can be accomplished when two DNA probes partly hybridize the target with the mismatched nucleotide being close to the nick between the two DNA probes and a ligase is used to close that nick. Only exact target-probe complementarity can result in stable ds DNA-RNA complexes, which can then be specifically detected by distinct Tb-dye FRET probes for multiplexed quantification of miRs at sub-nanomolar concentrations in serum-containing samples (**Figure 5A**).³⁵ When attaching DNAs to QD, the valency (number of DNA strands per QD) must be well adjusted. Whereas a high valency is beneficial for many hybridization and FRET events per QD, too many DNAs in close distance may interfere with target hybridization. When polyhistidine-appended DNA is used for DNA-QD selfassembly, valency can be controlled by adjusting the respective DNA and QD concentrations.^{28,29} Another possibility is the use of biotinylated DNA and QDs with a limited amount of streptavidin on their surface.^{28,37,50} An enzyme-free multiplexed assay could be realized by attaching short DNA probes on the surfaces of different QDs and exploiting the combination of base-pairing and base-stacking, which allowed the Tb-DNA to hybridize to the QD-DNA only when the specific miR target was present in the sample. Although color multiplexing was more straightforward when using the narrow PL spectra of the QDs, the simpler assay format and the larger Tb-to-QD distances led to slightly lower sensitivities in the low nanomolar concentration range (**Figure 5B**).³⁷ Detection of much lower concentrations can be accomplished by isothermal DNA amplification, such as rolling circle amplification (RCA).^{2,36} RCA-TG-FRET could be used to distinguish wild-type (WT) and single-point mutated (MT) dsDNA in the *BRAF* gene for liquid biopsy cancer diagnostics (**Figure 5C**).³⁸ Amplified Tb-to-dye TG-FRET duplexing could quantify the two WT and MT dsDNAs from a single sample in a 75 fM to 4.5 pM concentration range.

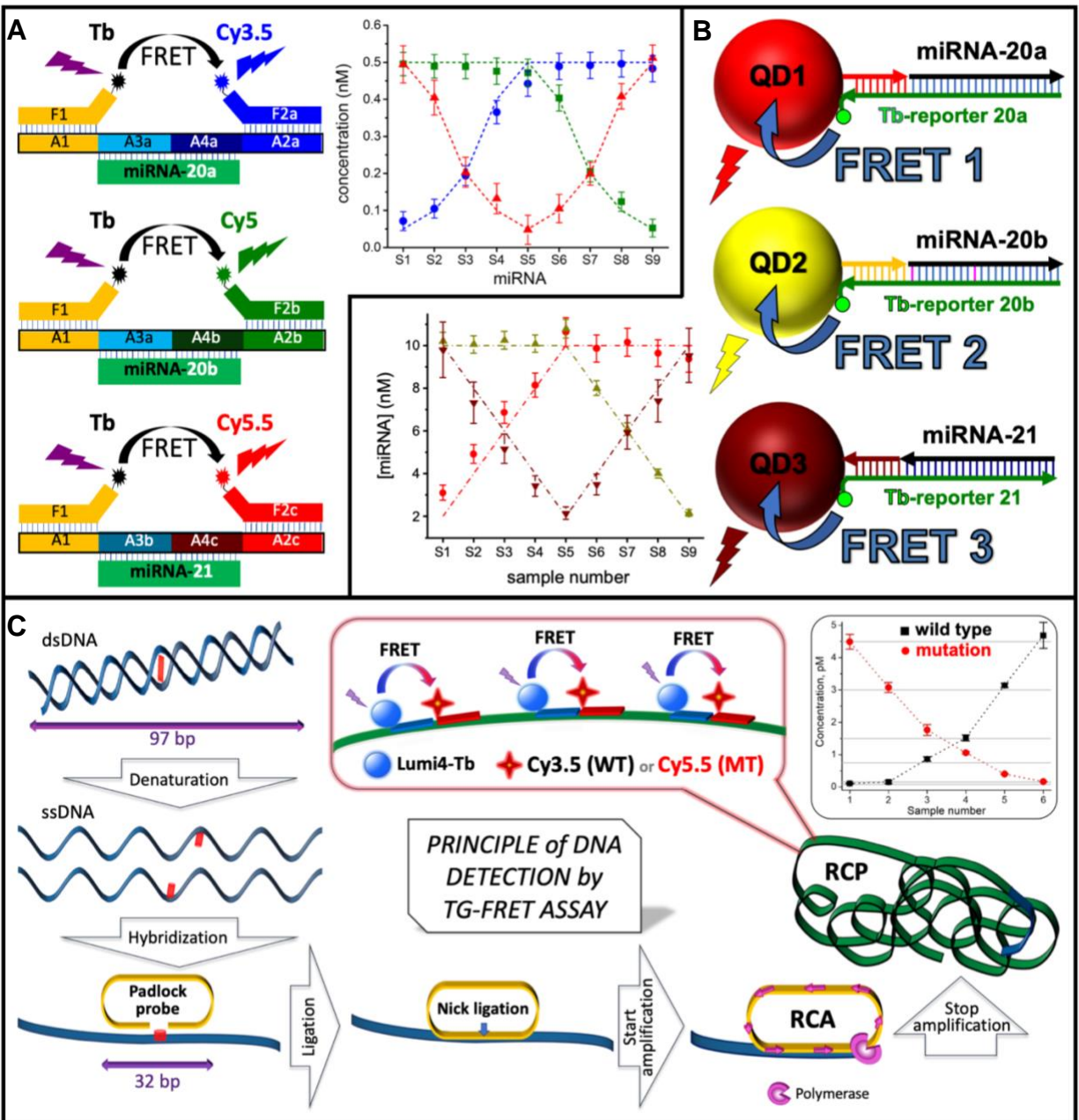


Figure 5. TG-FRET color multiplexing for RNA/DNA hybridization assays. (A) Specific hybridization of two adaptor oligos on different miRNA targets followed by ligation brings specific FRET DNA probes in close proximity for multiplexed TG-FRET quantification of the three miRNAs (graph shows the analysis of nine samples with different miRNA concentrations). Reproduced with permission from ref. 35. Copyright 2015 Wiley. (B) Target-specific Tb-DNA/QD-DNA hybridization resulted in TG-FRET, which could be used for triplexed miRNA quantification (graph shows the analysis of nine samples with different miRNA concentrations). Reproduced with permission from ref. 37. Copyright 2015 American Chemical Society. (C) After denaturation of dsDNA WT and MT targets, specific hybridization with a padlock probe, ligation, and target-primed RCA results in a long RCA product (RCP). Tb-dye FRET DNA-probes can hybridize to specific positions in the RCP to efficiently distinguish WT and MT dsDNA (graph shows the analysis of six samples with different DNA target concentrations). Reproduced with permission from ref. 38. Copyright 2019 American Chemical Society.

4.2 Temporally multiplexed DNA/RNA assays

The base-by-base distance tuning capability of nucleic acids is of particular advantage for temporal multiplexing. The first proof of concept system consisted of simple hybridization of two Tb and Cy5.5-terminated ssDNAs with different sequence lengths, such that the dsDNA would lead to distinct donor-acceptor distances (**Figure 1C**). Triplexed dsDNA quantification within a 0.5 nM to 2.5 nM concentration range was accomplished by measuring the PL intensities from three distinct temporal detection windows. The same study demonstrated duplexed quantification of miRs with only two base-pair mismatches using a single Tb-QD FRET pair with two distinct donor-acceptor distances (7.4 nm and 9.4 nm) and two temporal detection windows.²⁸

Applying temporal multiplexing to DNA-amplified sensors presents an efficient way to detect very low concentrations of nucleic acid biomarkers. Tb-to-Cy5.5 TG-FRET multiplexing was implemented in two enzyme-free amplification approaches (hybridization chain reaction, HCR - **Figure 6A**; catalytic hairpin assembly, CHA - **Figure 6B**) to quantify miR-20a and miR-21 from a single sample.^{39,40} Using hairpin probes with Tb and Cy5.5 labeled at different sequence positions, the amplified HCR or CHA products resulted in Tb-Cy5.5 distances of ~4.3 nm and ~5.2 nm for HCR and ~4.2 nm and ~5.1 nm for CHA, as determined by PL lifetime analysis, taking advantage of the FRET molecular ruler. Both techniques could perform duplexed miR quantification in a circa 30 pM to 400 pM concentration range (**Figures 6C and 6D**) and CHA could quantify both miRs at low picomolar concentrations from total RNA extracts of five different human tissue samples, demonstrating the actual applicability for clinical testing.

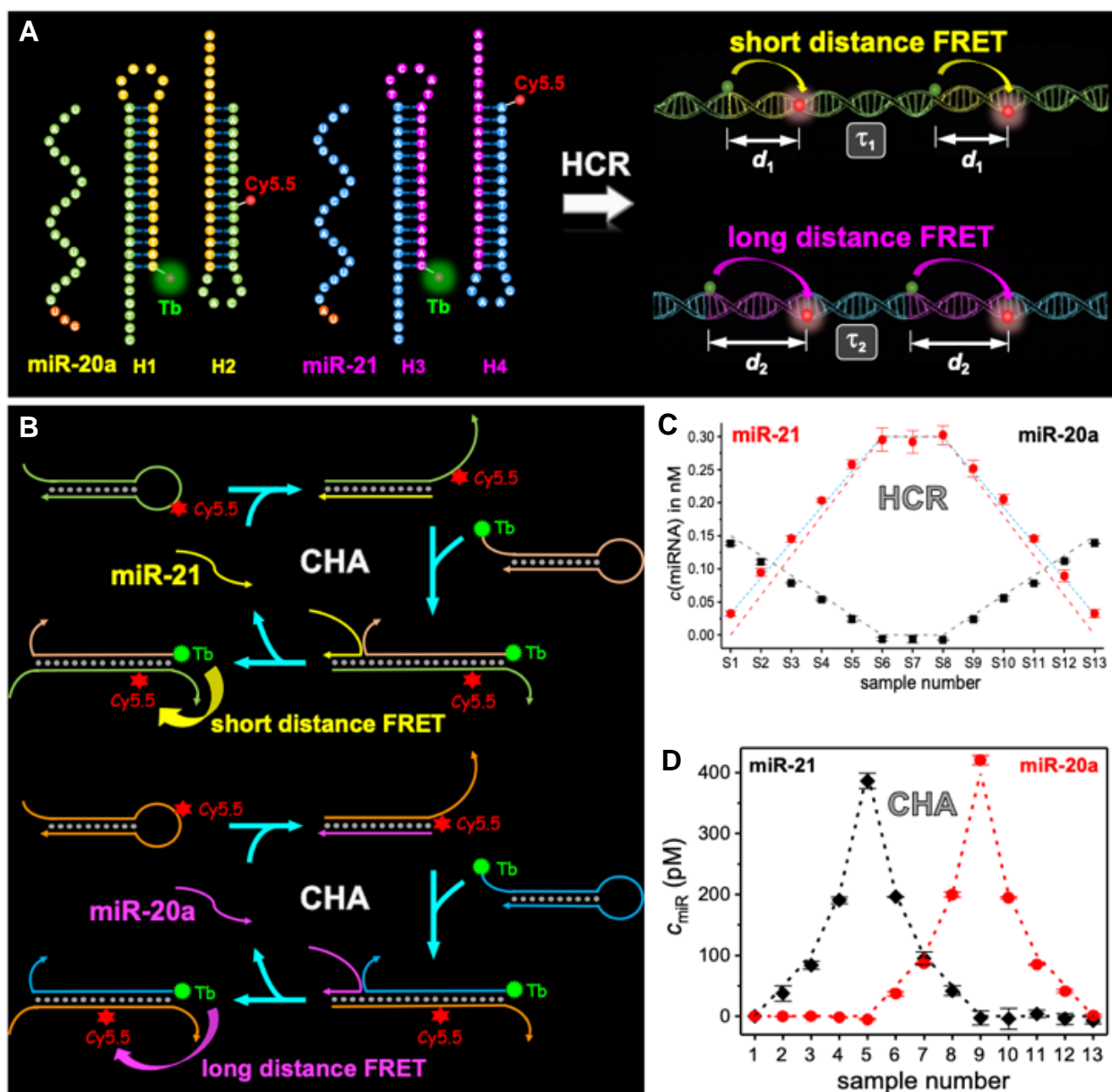


Figure 6. TG-FRET temporal multiplexing for RNA/DNA hybridization assays. Both HCR (A) and CHA (B) are based on two pairs of hairpin probes that contain Tb donors and Cy5.5 acceptors at distinct positions. The target-specifically amplified products result in multiple FRET pairs at two distinct distances. Thus, short and long distance FRET with a single FRET pair can be used for duplexed miR quantification (C for HCR and D for CHA). A and C reproduced with permission from ref. 39. Copyright 2019 American Chemical Society. B and D reproduced with permission from ref. 40. Copyright 2019 American Chemical Society.

4.3 Spectrotemporally multiplexed DNA/RNA assays

Isothermal target-primed RCA-TG-FRET provides extremely high DNA and RNA target selectivity and femtomolar LODs for the application to a broader range of clinical samples, including cells, blood, and tissues.^{36,38} On the other hand, the relatively complicated sensing format

may require optimization adapted to the sensing conditions, in particular when RCA-TG-FRET is combined with QDs.⁵⁰ In terms of spectral and temporal TG-FRET multiplexing, the repetitive sequence of the target-specific RCA product (RCP) can be used to hybridize many fluorescent DNA probes with different sequence lengths and fluorophores at distinct positions. Thus, amplification (many FRET pairs within one RCP), spectral multiplexing (one Tb donor combined with different dye acceptors), and temporal multiplexing (different Tb-dye distances) can be implemented in a single RCA-TG-FRET sensor (**Figure 7**). The combination of two FRET pairs with two temporal detection channels each was used for quadruplexed detection of four ssDNA targets at sub-picomolar concentrations.²

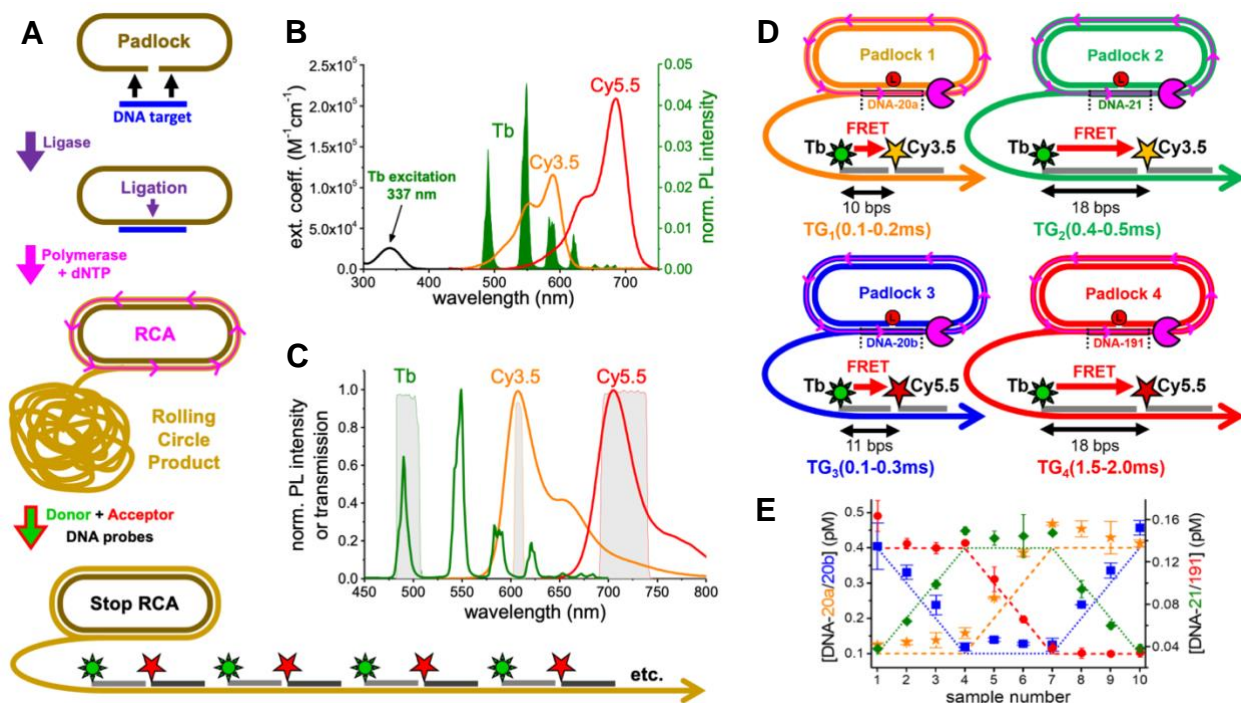


Figure 7. TG-FRET spectrotemporal multiplexing for RNA/DNA hybridization assays. (A) Each DNA target is hybridized by a specific padlock probe followed by RCA. The RCP is hybridized by Tb-donor and dye-acceptor DNA probes. (B) Spectra of Tb absorption (black) and emission (green) that partly overlaps with the absorption of Cy3.5 (orange) and Cy5.5 (red). (C) Emission spectra of Tb, Cy3.5, and Cy5.5. Optical bandpass filter transmission spectra (color detection channels) are shown in gray. (D) Two FRET pairs (Tb-Cy3.5 and Tb-Cy5.5) and two different donor-acceptor distances (shown in bps) provide four distinguishable signals (TG₁ to TG₄: two distinct TG detection windows for each color). (E) Recovery of varying target concentrations from 10 different samples using spectrotemporal TG-FRET multiplexing. Dotted lines represent known concentrations; data points represent RCA-TG-FRET measurements. Reproduced with permission from ref. 2. Copyright 2018 American Chemical Society.

5. TG-FRET IMAGING

Imaging detectors consist of an array of thousands of small sensors, each of which must capture a sufficient amount of photons to create the overall image. Because the photon flux (photons per time) is low for lanthanides compared to dyes (1 ms PL lifetime corresponds to ~1000 excitation-emission cycles per second, whereas 1 ns corresponds to ~1000 million cycles), lanthanide based imaging at similar fluorophore densities and signal integration times is always less bright. However, autofluorescence (noise) of cell or tissue samples is most often extremely bright for conventional detection and almost negligible for TG detection. Thus, when there is sufficient lanthanide PL, signal-to-noise ratios (the decisive measure for sensing and imaging) can become similar or even better for long PL lifetime TG imaging with the additional benefits of photostability, long-distance FRET, and multiplexing. Several recent studies have demonstrated the impressive capabilities of TG-FRET live-cell and *in-vivo* imaging.^{4,51,52}

5.1 Optical barcoding

Cellular and molecular barcoding has become an important method for a better understanding of multiple time-dependent processes and interactions in developmental biology and gene function.^{53–55} Temporal TG-FRET multiplexing has the potential to increase the fluorescence multiplexing capability by combining lanthanides, dyes, and QDs within single hybrid nanoparticles.^{3,30} Attachment of lanthanide complexes and dyes on QDs with a SiO₂ coating activates several different FRET channels between the various fluorophores, which can be adjusted by the SiO₂ coating thickness, the photophysical properties of the fluorophores, and their density on the surface (**Figure 8A**). The different spectral overlaps and distances between the fluorophores determine the FRET efficiencies and the concomitant PL lifetimes of FRET donors and acceptors. For example, the attachment of Eu or Tb complexes on QDs with two different SiO₂ coating thicknesses resulted in four distinct QD PL decays, all of which provided distinct intensities in three temporal detection windows that were encoded as red (R), green (G), and blue (B). Thus, the different intensity fractions in those three detection windows produced a unique RGB code for each of the four nanohybrids. When different cells were incubated with one type of nanohybrid, they could be efficiently distinguished in a mixture by recording a TG image in each detection window and overlaying them to an RGB image (**Figure 8B**).³⁰ The drawback of very different brightnesses of those purely temporally multiplexed codes could be overcome by co-assembling different amounts of Tb complexes and dyes on the same QD. While the Tb density mainly adjusted the QD PL

intensity, the dye density influenced both PL decay time and intensity of the QDs. The combination of three nanohybrids (10Tb/QD, 30Tb/QD/10dye, and 60Tb/QD/40dye) with three TG detection windows (R: 0.05 - 0.5 ms; G: 0.5 - 1.0 ms; and B: 1.0 - 4.0 ms) resulted in brightness-equalized codes that could be used to distinguish microbeads from a single overlay image (**Figure 8C**).³

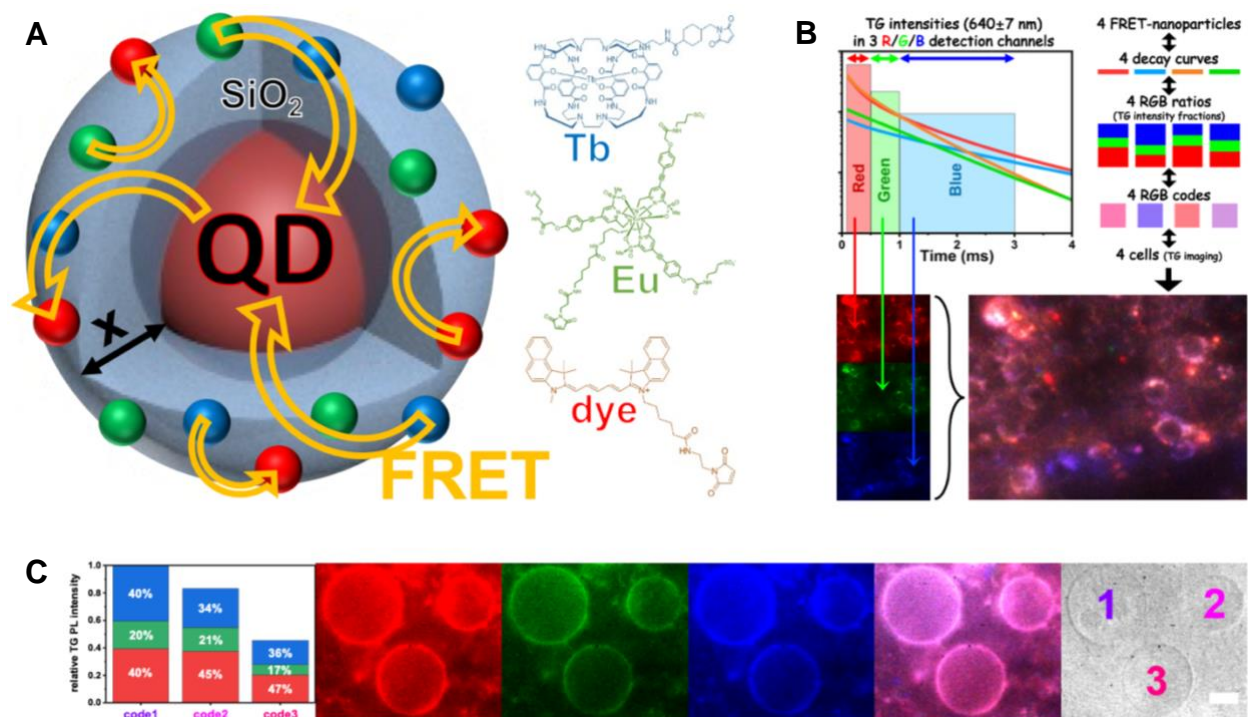


Figure 8. Optical barcoding via TG-FRET multiplexing. (A) Adjusting the density of Tb/Eu complexes and dyes on the surface of SiO₂ coated QDs (x : adjustable thickness) results in various tunable FRET processes. (B) PL decay curves of four TG-FRET nanoparticles (Tb-QD and Eu-QD with $x = 6$ nm or 12 nm) in three TG-detection windows give rise to RGB ratios specific to each type of nanoprobe. The four RGB codes were used to distinguish cells containing one of the four nanoprobe within one field of view by overlaying the three RGB images. (C) Co-attaching specific amounts of Tb complexes and dyes on a QD was used to produce temporally multiplexed nanohybrids with similar brightnesses, such that all luminescent barcodes could be imaged (microbeads with three different nanohybrids in R, G, B, and overlay images) with a single measurement without contrast adjustment. A and C adapted with permission from ref. 30. Copyright 2018 Wiley. A and C adapted with permission from ref. 3. Copyright 2019 American Chemical Society.

5.2. In-situ, in-vitro, and in-vivo imaging

TG-FRET amplification and nanohybrids can also be applied for imaging biomolecules and their interactions in living cells, tissues, and developing organisms, where FRET multiplexing at high signal-to-noise ratios and with high photostability is extremely important.⁵⁶ For example, intracellular actin could be detected on the single protein level via *in-situ* RCA-TG-FRET coupled to immunochemistry (**Figure 9A**).⁵⁷ Because TG-FRET could only occur in the amplified RCP

(hybridization of both Tb-DNA and dye-DNA), the signal per actin was both strongly amplified and very specific, thereby not interfering with background signals and avoiding any washing steps (**Figure 9B**). Wash-free and autofluorescence-free imaging with simple sample preparation and the capability of higher-order multiplexing has the potential to become very useful for sensitive imaging of intra- and extracellular biomarkers in clinical diagnostics.

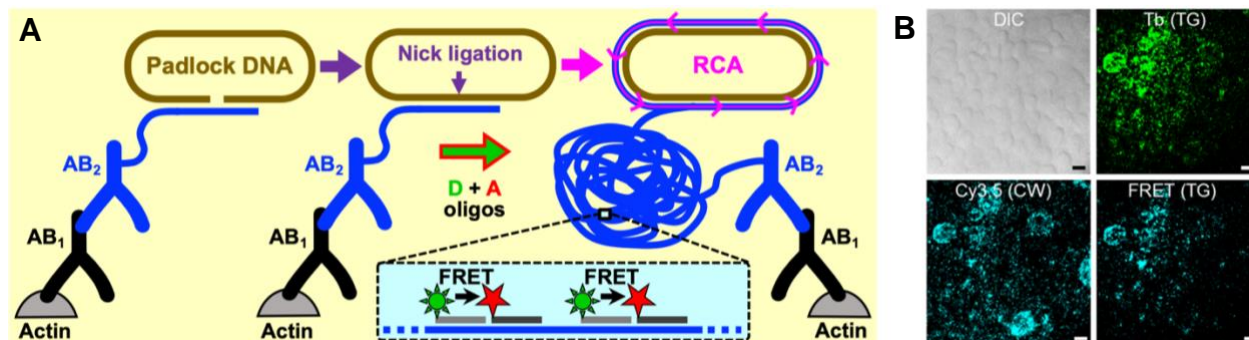


Figure 9. *In-situ* RCA-TG-FRET for washing-free imaging of single actin proteins. (A) Schematic assay protocol, including immunochemistry, RCA, and incubation with Tb-DNA and dye-DNA FRET probes. (B) β -actin expressed in HaCaT cells could be detected via TG-FRET after permeabilization, RCA protocol, and few minutes of incubation with the FRET DNA probes. TG-FRET provided more specific and background-free signals compared to TG Tb PL and continuous wave (CW) Cy3.5 dye PL without washing the cells after probe incubation. Scale bars: 10 μ m. Reproduced with permission from ref. 57. Copyright 2020 American Chemical Society.

The multiplexing advantages of TG-FRET nanohybrids can be further exploited for live-cell imaging and detecting intracellular biomolecular interactions. For such applications, peptides and proteins can be attached to QDs to induce various FRET processes between QDs, lanthanide complexes, dyes, and fluorescent proteins (FPs) (**Figure 10A**).^{4,58} The versatility and multiplexing capability for autofluorescence-free imaging was demonstrated via *i*) triplexed intracellular TG-FRET between a Tb complex and three different QDs (**Figure 10B**),⁴ *ii*) multistep intracellular TG-FRET from Tb-to-QD-to-dye (**Figure 10C**),⁵⁸ and *iii*) multistep TG-FRET from Tb-to-QD-to-FP to monitor the intracellular attachment of transiently expressed FP to the TG-FRET nanohybrids (**Figure 10D**).⁴ Beyond multiplexing, the outstanding signal-to-noise ratios and photostability of TG-FRET nanohybrids could be used for long-term imaging in a developing organism. After microinjection of concentrated nanoprobe (few μ M) in zebrafish embryos at the one-cell stage, autofluorescence-free *in-vivo* imaging could be performed for up to seven days (**Figure 10E**). This long-term imaging capability showed that even after an extreme increase in cell number and volume of the zebrafish larvae, the initially injected TG-FRET-nanohybrids still emitted bright PL.

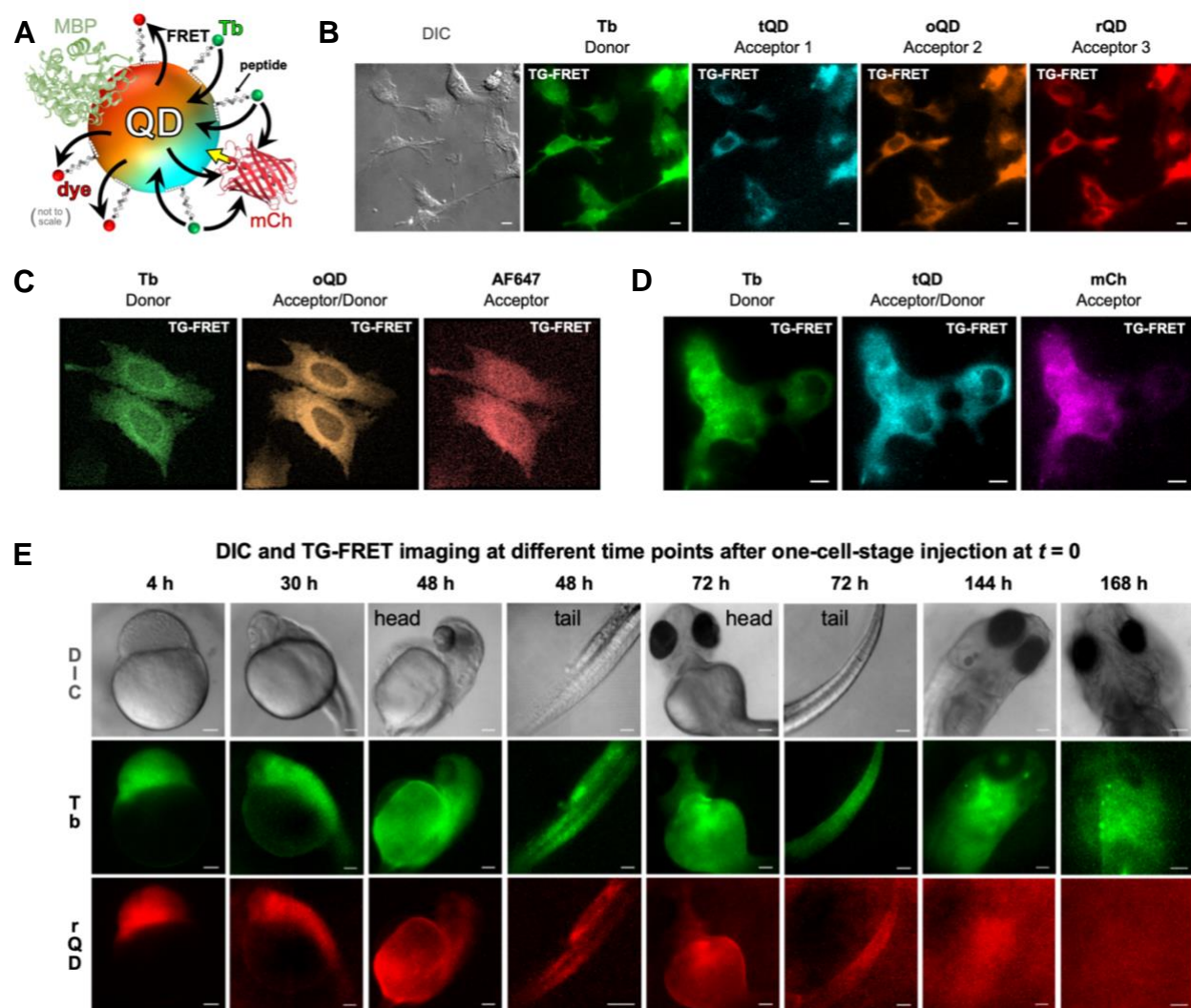


Figure 10. Live-cell and *in-vivo* TG-FRET imaging. (A) TG-FRET nanohybrids consist of a central QD, to which different peptides, proteins, and FRET donors/acceptors can be attached for multiplexed sensing design. (B) Four-color TG-FRET imaging of COS-7 cells microinjected with Tb-QD nanoprobe composed of turquoise (tQD), orange (oQD), and red (rQD) QDs. (C) Three-color imaging of intracellular multistep TG-FRET from Tb-to-QD-to-dye (Alexa Fluor 647: AF647). (D) Three-color imaging of multistep TG-FRET from Tb-to-QD-to-FP (mCherry: mCh) upon intracellular assembly of transiently expressed FPs to Tb-QD nanohybrids. (E) Long-term Tb-to-QD TG-FRET imaging in developing zebrafish embryos. Scale bars 10 μm (B, C, D) and 100 μm (E). C adapted with permission from ref. 58. Copyright 2016 The Authors, some rights reserved; exclusive licensee American Association for the Advancement of Science. Distributed under a Creative Commons Attribution License 4.0 (CC BY) <https://creativecommons.org/licenses/by/4.0/>. A, B, D, E adapted with permission from ref. 4. Copyright 2020 Wiley.

6. CONCLUSIONS AND OUTLOOK

TG-FRET using lanthanide donors with long PL lifetimes and various acceptors, such as dyes, QDs, or FPs, can significantly improve multiplexing capabilities in biosensing and bioimaging. Spectral, temporal, and spectrotemporal multiplexing within a single sample, efficient suppression of sample

autofluorescence, wash-free assay formats, and high photostability provide many opportunities for implementing TG-FRET into clinical diagnostics and bioanalytical research. TG-FRET can perform *in-vitro*, *in-situ*, and *in-vivo* analysis of low volume serum samples, living cells, tissues, and developing organisms with high spatial resolution, high selectivity, and high sensitivity. However, TG-FRET is only one of the many available tools and its benefits must always be weighed against its limitations (e.g., relatively low photon flux, few available probes, specialized setups for imaging), some of which present important challenges for future TG-FRET research. A perfect method with the best performance for all bioanalytical parameters does unfortunately not exist. Both analytical priority (e.g., sensitivity, specificity, multiplexing, simplicity) and available sensing technologies (e.g., optical, electrochemical, mass-based) for a specific application must be carefully considered during biosensor development. The discovery and understanding of more and more complicated biological systems comprising multiple parallel and sequential biomolecular interactions in clinical, molecular, developmental, and neuro biology will make multiplexed detection and imaging even more demanding and important in the future. Technical advances, new and better materials, smart multihybrid nanosystems, and interdisciplinary studies with the potential to implement sophisticated TG-FRET multiplexing probes into sophisticated biological systems will be important drivers for future applications and the translation of TG-FRET multiplexing into a standard technology for multi-level analysis in biosensing and bioimaging.

SUPPORTING INFORMATION

The Supporting Information is available free of charge at ...

Additional Information concerning size, orientation, conformation, and proximity for optimizing QD-based immunoassays (PDF)

BIOGRAPHIES

Xue Qiu (orcid.org/0000-0003-0635-6801) received her PhD in 2016 from University Paris-Saclay. From 2016 to 2019, she worked as research biologist at I2BC. Since 2020 she has been Full Professor at Ocean University of China. Xue's research interests are FRET based applications in drug discovery and biomedical engineering.

Jingyue Xu (orcid.org/0000-0002-9949-8536) received her Master degree from Jilin University in 2016 and her PhD from University Paris-Saclay in 2020. Her professional interests include the development of novel biosensing technologies and the application of FRET for sensitive and multiplexed detection and *in-vitro* diagnostics.

Marcelina Cardoso Dos Santos (orcid.org/0000-0003-2004-1777) received her PhD in 2015 from Université de Technologie de Troyes, after which she joined I2BC, where she became a permanent CEA researcher in 2018. She currently works at I2BC in the group of Christophe Le Clainche and develops FRET biosensors to study molecular assemblies in artificial cells.

Niko Hildebrandt (orcid.org/0000-0001-8767-9623) holds a PhD in Physical Chemistry (2007). He has been group leader at various institutes in Germany and France and Full Professor at Université Paris-Saclay since 2010. Currently, he is Guest Professor in the Department of Chemistry at Seoul National University. Niko's main research interests are luminescence spectroscopy and microscopy and the application of lanthanides and nanomaterials for multiplexed FRET biosensing.

ACKNOWLEDGEMENTS

This work has been supported by the Korean National Research Foundation, Seoul National University, the National Natural Science Foundation of China (No. 82104120), Université Paris-Saclay, Université de Rouen Normandie, INSA Rouen, CNRS, European Regional Development Fund, Labex SynOrg (ANR-11-LABX-0029), Carnot Institute I2C, XL-Chem graduate school (ANR-18-EURE-0020 XL CHEM), the Region Normandie, Institut Universitaire de France, and the China Scholarship Council.

REFERENCES

- (1) Léger, C.; Yahia-Ammar, A.; Susumu, K.; Medintz, I. L.; Urvoas, A.; Valerio-Lepiniec, M.; Minard, P.; Hildebrandt, N. Picomolar Biosensing and Conformational Analysis Using Artificial Bidomain Proteins and Terbium-to-Quantum Dot Förster Resonance Energy Transfer. *ACS Nano* **2020**, *14*, 5956–5967. <https://doi.org/10.1021/acsnano.0c01410>.
- (2) Qiu, X.; Guo, J.; Xu, J.; Hildebrandt, N. Three-Dimensional FRET Multiplexing for DNA Quantification with Attomolar Detection Limits. *J. Phys. Chem. Lett.* **2018**, *9*, 4379–4384. <https://doi.org/10.1021/acs.jpcllett.8b01944>.

- (3) Chen, C.; Corry, B.; Huang, L.; Hildebrandt, N. FRET-Modulated Multihybrid Nanoparticles for Brightness-Equalized Single-Wavelength Barcoding. *J. Am. Chem. Soc.* **2019**, *141*, 11123–11141. <https://doi.org/10.1021/jacs.9b03383>.
- (4) Cardoso Dos Santos, M.; Colin, I.; Ribeiro Dos Santos, G.; Susumu, K.; Demarque, M.; Medintz, I. L.; Hildebrandt, N. Time-Gated FRET Nanoprobes for Autofluorescence-Free Long-Term In Vivo Imaging of Developing Zebrafish. *Adv. Mater.* **2020**, *32*, 2003912. <https://doi.org/10.1002/adma.202003912>.
- (5) Becquerel, E. Chapitre II: Durée et Intensité de La Lumière Émise. In *La lumière, ses causes, ses effets. Tome premier: Sources de lumière*; Librairie de Firmin Didot Frères: Paris, 1867; pp 244–298.
- (6) Cario, G.; Franck, J. Über Zerlegung von Wasserstoffmolekülen durch angeregte Quecksilberatome. *Z. Physik* **1922**, *11*, 161–166. <https://doi.org/10.1007/BF01328410>.
- (7) Morrison, L. E. Time-Resolved Detection of Energy Transfer: Theory and Application to Immunoassays. *Anal. Biochem.* **1988**, *174*, 101–120. [https://doi.org/10.1016/0003-2697\(88\)90524-6](https://doi.org/10.1016/0003-2697(88)90524-6).
- (8) Hemmila, I. LANCE™: Homogeneous Assay Platform for HTS. *J. Biomol. Screen.* **1999**, *4*, 303–307. <https://doi.org/10.1177/108705719900400604>.
- (9) Ju, J.; Ruan, C.; Fuller, C. W.; Glazer, A. N.; Mathies, R. A. Fluorescence Energy Transfer Dye-Labeled Primers for DNA Sequencing and Analysis. *Proc. Natl. Acad. Sci. USA* **1995**, *92*, 4347–4351. <https://doi.org/10.1073/pnas.92.10.4347>.
- (10) Heim, R.; Tsien, R. Y. Engineering Green Fluorescent Protein for Improved Brightness, Longer Wavelengths and Fluorescence Resonance Energy Transfer. *Curr. Biol.* **1996**, *6*, 178–182. [https://doi.org/10.1016/S0960-9822\(02\)00450-5](https://doi.org/10.1016/S0960-9822(02)00450-5).
- (11) Ha, T.; Enderle, T.; Ogletree, D. F.; Chemla, D. S.; Selvin, P. R.; Weiss, S. Probing the Interaction between Two Single Molecules: Fluorescence Resonance Energy Transfer between a Single Donor and a Single Acceptor. *Proc. Natl. Acad. Sci. USA* **1996**, *93*, 6264–6268. <https://doi.org/10.1073/pnas.93.13.6264>.
- (12) Hildebrandt, N.; Spillmann, C. M.; Algar, W. R.; Pons, T.; Stewart, M. H.; Oh, E.; Susumu, K.; Díaz, S. A.; Delehanty, J. B.; Medintz, I. L. Energy Transfer with Semiconductor Quantum Dot Bioconjugates: A Versatile Platform for Biosensing, Energy Harvesting, and Other Developing Applications. *Chem. Rev.* **2017**, *117*, 536–711. <https://doi.org/10.1021/acs.chemrev.6b00030>.
- (13) Algar, W. R.; Massey, M.; Rees, K.; Higgins, R.; Krause, K. D.; Darwish, G. H.; Peveler, W. J.; Xiao, Z.; Tsai, H.-Y.; Gupta, R.; Lix, K.; Tran, M. V.; Kim, H. Photoluminescent Nanoparticles for Chemical and Biological Analysis and Imaging. *Chem. Rev.* **2021**, *121*, 9243–9358. <https://doi.org/10.1021/acs.chemrev.0c01176>.
- (14) Hildebrandt, N.; Wegner, K. D.; Algar, W. R. Luminescent Terbium Complexes: Superior Förster Resonance Energy Transfer Donors for Flexible and Sensitive Multiplexed Biosensing. *Coord. Chem. Rev.* **2014**, *273–274*, 125–138. <https://doi.org/10.1016/j.ccr.2014.01.020>.
- (15) Cardoso Dos Santos, M.; Algar, W. R.; Medintz, I. L.; Hildebrandt, N. Quantum Dots for Förster Resonance Energy Transfer (FRET). *TrAC Trends Anal. Chem.* **2020**, *125*, 115819. <https://doi.org/10.1016/j.trac.2020.115819>.
- (16) Zwier, J. M.; Hildebrandt, N. Time-Gated FRET Detection for Multiplexed Biosensing. In *Reviews in Fluorescence 2016*; Geddes, CD, Ed.; Reviews in Fluorescence; Springer, Cham, 2017; pp 17–43. https://doi.org/10.1007/978-3-319-48260-6_3.
- (17) Qiu, X.; Hildebrandt, N. A Clinical Role for Förster Resonance Energy Transfer in Molecular Diagnostics of Disease. *Expert Rev. Mol. Diagn.* **2019**, *19*, 767–771. <https://doi.org/10.1080/14737159.2019.1649144>.

- (18) Algar, W. R.; Hildebrandt, N.; Vogel, S. S.; Medintz, I. L. FRET as a Biomolecular Research Tool — Understanding Its Potential While Avoiding Pitfalls. *Nat. Methods* **2019**, *16*, 815–829. <https://doi.org/10.1038/s41592-019-0530-8>.
- (19) Zhang, R.; Yuan, J. Responsive Metal Complex Probes for Time-Gated Luminescence Biosensing and Imaging. *Acc. Chem. Res.* **2020**, *53*, 1316–1329. <https://doi.org/10.1021/acs.accounts.0c00172>.
- (20) Sørensen, T. J.; Faulkner, S. 5 Lanthanide Complexes Used for Optical Imaging. In *Metal Ions in Bio-Imaging Techniques*; Sigel, A., Freisinger, E., Sigel, R. K. O., Eds.; De Gruyter Berlin, 2021. <https://doi.org/10.1515/9783110685701-011>.
- (21) Hildebrandt, N. How to Apply FRET: From Experimental Design to Data Analysis. In *FRET – Förster Resonance Energy Transfer*; Medintz, I. L., Hildebrandt, N., Eds.; Wiley-VCH Verlag GmbH & Co. KGaA, Weinheim, 2013; pp 105–163. <https://doi.org/10.1002/9783527656028.ch05>.
- (22) Hermanson, G. T. *Bioconjugate Techniques*, 3rd ed.; Academic Press, 2013.
- (23) Krall, N.; da Cruz, F. P.; Boutureira, O.; Bernardes, G. J. L. Site-Selective Protein-Modification Chemistry for Basic Biology and Drug Development. *Nat. Chem.* **2016**, *8*, 103–113. <https://doi.org/10.1038/nchem.2393>.
- (24) Rashidian, M.; Dozier, J. K.; Distefano, M. D. Enzymatic Labeling of Proteins: Techniques and Approaches. *Bioconjugate Chem.* **2013**, *24*, 1277–1294. <https://doi.org/10.1021/bc400102w>.
- (25) Bernardim, B.; Cal, P. M. S. D.; Matos, M. J.; Oliveira, B. L.; Martínez-Sáez, N.; Albuquerque, I. S.; Perkins, E.; Corzana, F.; Burtoloso, A. C. B.; Jiménez-Osés, G.; Bernardes, G. J. L. Stoichiometric and Irreversible Cysteine-Selective Protein Modification Using Carbonylacrylic Reagents. *Nat. Commun.* **2016**, *7*, 13128. <https://doi.org/10.1038/ncomms13128>.
- (26) Kovacs, D.; Lu, X.; Mészáros, L. S.; Ott, M.; Andres, J.; Borbas, K. E. Photophysics of Coumarin and Carbostyryl-Sensitized Luminescent Lanthanide Complexes: Implications for Complex Design in Multiplex Detection. *J. Am. Chem. Soc.* **2017**, *139*, 5756–5767. <https://doi.org/10.1021/jacs.6b11274>.
- (27) Geißler, D.; Stufler, S.; Löhmansröben, H.-G.; Hildebrandt, N. Six-Color Time-Resolved Förster Resonance Energy Transfer for Ultrasensitive Multiplexed Biosensing. *J. Am. Chem. Soc.* **2013**, *135*, 1102–1109. <https://doi.org/10.1021/ja310317n>.
- (28) Qiu, X.; Guo, J.; Jin, Z.; Petreto, A.; Medintz, I. L.; Hildebrandt, N. Multiplexed Nucleic Acid Hybridization Assays Using Single-FRET-Pair Distance-Tuning. *Small* **2017**, *13*, 1700332. <https://doi.org/10.1002/sml.201700332>.
- (29) Guo, J.; Qiu, X.; Mingoies, C.; Deschamps, J. R.; Susumu, K.; Medintz, I. L.; Hildebrandt, N. Conformational Details of Quantum Dot-DNA Resolved by Förster Resonance Energy Transfer Lifetime Nanoruler. *ACS Nano* **2019**, *13*, 505–514. <https://doi.org/10.1021/acsnano.8b07137>.
- (30) Chen, C.; Ao, L.; Wu, Y.-T.; Cifliku, V.; Cardoso Dos Santos, M.; Bourrier, E.; Delbianco, M.; Parker, D.; Zwier, J. M.; Huang, L.; Hildebrandt, N. Single-Nanoparticle Cell Barcoding by Tunable FRET from Lanthanides to Quantum Dots. *Angew. Chem. Int. Ed.* **2018**, *57*, 13686–13690. <https://doi.org/10.1002/anie.201807585>.
- (31) Geißler, D.; Charbonnière, L. J.; Ziessel, R. F.; Butlin, N. G.; Löhmansröben, H.-G.; Hildebrandt, N. Quantum Dot Biosensors for Ultrasensitive Multiplexed Diagnostics. *Angew. Chem. Int. Ed.* **2010**, *49*, 1396–1401. <https://doi.org/10.1002/anie.200906399>.
- (32) Xiong, R.; Mara, D.; Liu, J.; Van Deun, R.; Borbas, K. E. Excitation- and Emission-Wavelength-Based Multiplex Spectroscopy Using Red-Absorbing Near-Infrared-Emitting Lanthanide Complexes. *J. Am. Chem. Soc.* **2018**, *140*, 10975–10979. <https://doi.org/10.1021/jacs.8b07609>.
- (33) Carro-Temboury, M. R.; Arppe, R.; Vosch, T.; Sørensen, T. J. An Optical Authentication System Based on Imaging of Excitation-Selected Lanthanide Luminescence. *Sci. Adv.* **2018**, *4*, e1701384. <https://doi.org/10.1126/sciadv.1701384>.

- (34) Bhuckory, S.; Wegner, K. D.; Qiu, X.; Wu, Y.-T.; Jennings, T. L.; Incamps, A.; Hildebrandt, N. Triplexed CEA-NSE-PSA Immunoassay Using Time-Gated Terbium-to-Quantum Dot FRET. *Molecules* **2020**, *25*, 3679. <https://doi.org/10.3390/molecules25163679>.
- (35) Jin, Z.; Geissler, D.; Qiu, X.; Wegner, K. D.; Hildebrandt, N. A Rapid, Amplification-Free, and Sensitive Diagnostic Assay for Single-Step Multiplexed Fluorescence Detection of MicroRNA. *Angew. Chem. Int. Ed.* **2015**, *54*, 10024–10029. <https://doi.org/10.1002/anie.201504887>.
- (36) Qiu, X.; Xu, J.; Guo, J.; Yahia-Ammar, A.; Kapetanakis, N.-I.; Duroux-Richard, I.; Unterluggauer, J. J.; Golob-Schwarzl, N.; Regeard, C.; Uzan, C.; Gouy, S.; DuBow, M.; Haybaeck, J.; Apparailly, F.; Busson, P.; Hildebrandt, N. Advanced MicroRNA-Based Cancer Diagnostics Using Amplified Time-Gated FRET. *Chem. Sci.* **2018**, *9*, 8046–8055. <https://doi.org/10.1039/c8sc03121e>.
- (37) Qiu, X.; Hildebrandt, N. Rapid and Multiplexed MicroRNA Diagnostic Assay Using Quantum Dot-Based Förster Resonance Energy Transfer. *ACS Nano* **2015**, *9*, 8449–8457. <https://doi.org/10.1021/acs.nano.5b03364>.
- (38) Dekaliuk, M.; Qiu, X.; Troalen, F.; Busson, P.; Hildebrandt, N. Discrimination of the V600E Mutation in BRAF by Rolling Circle Amplification and Förster Resonance Energy Transfer. *ACS Sens.* **2019**, *4*, 2786–2793. <https://doi.org/10.1021/acssensors.9b01420>.
- (39) Guo, J.; Mingoies, C.; Qiu, X.; Hildebrandt, N. Simple, Amplified, and Multiplexed Detection of MicroRNAs Using Time-Gated FRET and Hybridization Chain Reaction. *Anal. Chem.* **2019**, *91*, 3101–3109. <https://doi.org/10.1021/acs.analchem.8b05600>.
- (40) Xu, J.; Guo, J.; Golob-Schwarzl, N.; Haybaeck, J.; Qiu, X.; Hildebrandt, N. Single-Measurement Multiplexed Quantification of MicroRNAs from Human Tissue Using Catalytic Hairpin Assembly and Förster Resonance Energy Transfer. *ACS Sens.* **2020**, *5*, 1768–1776. <https://doi.org/10.1021/acssensors.0c00432>.
- (41) Qiu, X.; Wegner, K. D.; Wu, Y.-T.; Henegouwen, P. M. P. van B. en; Jennings, T. L.; Hildebrandt, N. Nanobodies and Antibodies for Duplexed EGFR/HER2 Immunoassays Using Terbium-to-Quantum Dot FRET. *Chem. Mater.* **2016**, *28*, 8256–8267. <https://doi.org/10.1021/acs.chemmater.6b03198>.
- (42) Wegner, K. D.; Jin, Z.; Linden, S.; Jennings, T. L.; Hildebrandt, N. Quantum-Dot-Based Förster Resonance Energy Transfer Immunoassay for Sensitive Clinical Diagnostics of Low-Volume Serum Samples. *ACS Nano* **2013**, *7*, 7411–7419. <https://doi.org/10.1021/nn403253y>.
- (43) Bhuckory, S.; Lefebvre, O.; Qiu, X.; Wegner, K. D.; Hildebrandt, N. Evaluating Quantum Dot Performance in Homogeneous FRET Immunoassays for Prostate Specific Antigen. *Sensors* **2016**, *16*, 197. <https://doi.org/10.3390/s16020197>.
- (44) Mattera, L.; Bhuckory, S.; Wegner, K. D.; Qiu, X.; Agnese, F.; Lincheneau, C.; Senden, T.; Djurado, D.; Charbonniere, L. J.; Hildebrandt, N.; Reiss, P. Compact Quantum Dot-Antibody Conjugates for FRET Immunoassays with Subnanomolar Detection Limits. *Nanoscale* **2016**, *8*, 11275–11283. <https://doi.org/10.1039/c6nr03261c>.
- (45) Sapsford, K. E.; Algar, W. R.; Berti, L.; Gemmill, K. B.; Casey, B. J.; Oh, E.; Stewart, M. H.; Medintz, I. L. Functionalizing Nanoparticles with Biological Molecules: Developing Chemistries That Facilitate Nanotechnology. *Chem. Rev.* **2013**, *113*, 1904–2074. <https://doi.org/10.1021/cr300143v>.
- (46) Morgner, F.; Geissler, D.; Stufler, S.; Butlin, N. G.; Loehmannsroeben, H.-G.; Hildebrandt, N. A Quantum-Dot-Based Molecular Ruler for Multiplexed Optical Analysis. *Angew. Chem. Int. Ed.* **2010**, *49*, 7570–7574. <https://doi.org/10.1002/anie.201002943>.
- (47) Wu, Y.-T.; Qiu, X.; Lindbo, S.; Susumu, K.; Medintz, I. L.; Hober, S.; Hildebrandt, N. Quantum Dot-Based FRET Immunoassay for HER2 Using Ultrasmall Affinity Proteins. *Small* **2018**, *14*, 1802266. <https://doi.org/10.1002/smll.201802266>.
- (48) Wegner, K. D.; Linden, S.; Jin, Z.; Jennings, T. L.; el Khoulati, R.; Henegouwen, P. M. P. van B. E.; Hildebrandt, N. Nanobodies and Nanocrystals: Highly Sensitive Quantum Dot-Based Homogeneous

- FRET Immunoassay for Serum-Based EGFR Detection. *Small* **2014**, *10*, 734–740. <https://doi.org/10.1002/sml.201302383>.
- (49) Bhuckory, S.; Mattera, L.; Wegner, K. D.; Qiu, X.; Wu, Y.-T.; Charbonniere, L. J.; Reiss, P.; Hildebrandt, N. Direct Conjugation of Antibodies to the ZnS Shell of Quantum Dots for FRET Immunoassays with Low Picomolar Detection Limits. *Chem. Commun.* **2016**, *52*, 14423–14425. <https://doi.org/10.1039/c6cc08835j>.
- (50) Xu, J.; Qiu, X.; Hildebrandt, N. When Nanoworlds Collide: Implementing DNA Amplification, Nanoparticles, Molecules, and FRET into a Single MicroRNA Biosensor. *Nano Lett.* **2021**, *21*, 4802–4808. <https://doi.org/10.1021/acs.nanolett.1c01351>.
- (51) Cho, U.; Riordan, D. P.; Ciepla, P.; Kocherlakota, K. S.; Chen, J. K.; Harbury, P. B. Ultrasensitive Optical Imaging with Lanthanide Lumiphores. *Nat. Chem. Biol.* **2018**, *14*, 15–21. <https://doi.org/10.1038/nchembio.2513>.
- (52) Chen, T.; Pham, H.; Mohamadi, A.; Miller, L. W. Single-Chain Lanthanide Luminescence Biosensors for Cell-Based Imaging and Screening of Protein-Protein Interactions. *iScience* **2020**, *23*, 101533. <https://doi.org/10.1016/j.isci.2020.101533>.
- (53) Kbschull, J. M.; Zador, A. M. Cellular Barcoding: Lineage Tracing, Screening and Beyond. *Nat. Methods* **2018**, *15*, 871–879. <https://doi.org/10.1038/s41592-018-0185-x>.
- (54) Askary, A.; Sanchez-Guardado, L.; Linton, J. M.; Chadly, D. M.; Budde, M. W.; Cai, L.; Lois, C.; Elowitz, M. B. In Situ Readout of DNA Barcodes and Single Base Edits Facilitated by in Vitro Transcription. *Nat. Biotechnol.* **2020**, *38*, 66–75. <https://doi.org/10.1038/s41587-019-0299-4>.
- (55) Zhang, J. Q.; Siltanen, C. A.; Liu, L.; Chang, K.-C.; Gartner, Z. J.; Abate, A. R. Linked Optical and Gene Expression Profiling of Single Cells at High-Throughput. *Genome Biol.* **2020**, *21*, 49. <https://doi.org/10.1186/s13059-020-01958-9>.
- (56) Bunt, G.; Wouters, F. S. FRET from Single to Multiplexed Signaling Events. *Biophys. Rev.* **2017**, *9*, 119–129. <https://doi.org/10.1007/s12551-017-0252-z>.
- (57) Francés-Soriano, L.; Leino, M.; Cardoso Dos Santos, M.; Kovacs, D.; Borbas, K. E.; Söderberg, O.; Hildebrandt, N. In Situ Rolling Circle Amplification Förster Resonance Energy Transfer (RCA-FRET) for Washing-Free Real-Time Single-Protein Imaging. *Anal. Chem.* **2021**, *93*, 1842–1850. <https://doi.org/10.1021/acs.analchem.0c04828>.
- (58) Afsari, H. S.; Cardoso Dos Santos, M.; Linden, S.; Chen, T.; Qiu, X.; Henegouwen, P. M. P. van B. E.; Jennings, T. L.; Susumu, K.; Medintz, I. L.; Hildebrandt, N.; Miller, L. W. Time-Gated FRET Nanoassemblies for Rapid and Sensitive Intra- and Extracellular Fluorescence Imaging. *Sci. Adv.* **2016**, *2*, e1600265. <https://doi.org/10.1126/sciadv.1600265>.